Mechanism of receptor-oriented intercellular calcium wave propagation in hepatocytes

GENEVIÈVE DUPONT,* THIERRY TORDJMANN,† CAROLINE CLAIR,† STÉPHANE SWILLENS,‡ MICHEL CLARET,† AND LAURENT COMBETTES†,[1]

*Université Libre de Bruxelles, Faculté des Sciences CP231, Brussels, Belgium; †Unité de Recherche U442, Institut National de la Santé et de la Recherche Médicale, Université de Paris sud, Orsay, France; and ‡Université Libre de Bruxelles, IRIBHN, Faculté de Médecine, Campus Erasme, Brussels, Belgium

ABSTRACT **Intercellular calcium signals are propagated in multicellular hepatocyte systems as well as in the intact liver. The stimulation of connected hepatocytes by glycogenolytic agonists induces reproducible sequences of intracellular calcium concentration increases, resulting in unidirectional intercellular calcium waves. Hepatocytes are characterized by a gradient of vasopressin binding sites from the periportal to perivenous areas of the cell plate in hepatic lobules. Also, coordination of calcium signals between neighboring cells requires the presence of the agonist at each cell surface as well as gap junction permeability. We present a model based on the junctional coupling of several hepatocytes differing in sensitivity to the agonist and thus in the intrinsic period of calcium oscillations. In this model, each hepatocyte displays repetitive calcium spikes with a slight phase shift with respect to neighboring cells, giving rise to a phase wave. The orientation of the apparent calcium wave is imposed by the direction of the gradient of hormonal sensitivity. Calcium spikes are coordinated by the diffusion across junctions of small amounts of inositol 1,4,5-trisphosphate ($InsP_3$). Theoretical predictions from this model are confirmed experimentally. Thus, major physiological insights may be gained from this model for coordination and spatial orientation of intercellular signals.—Dupont, G., Tordjmann, T., Clair, C., Swillens, S., Claret, M., Combettes, L. Mechanism of receptor-oriented intercellular calcium wave propagation in hepatocytes.** ***FASEB J.*** **14, 279–289 (2000)**

Key Words: liver · phase wave · gap junctions · inositol 1,4,5-trisphosphate

In the liver, many important physiological processes such as bile secretion, bile flow, glycogen breakdown, and cell survival are regulated by an increase in the level of cytosolic Ca^{2+} (1). These Ca^{2+} signals can be elicited in isolated cells by a large array of stimuli and often occur as repetitive Ca^{2+} waves. The regenerative mechanism of these Ca^{2+} waves is beginning to be well understood (2). In isolated multicellular systems, or in intact organs, Ca^{2+} waves are not restricted to the cytosol of one cell but propagate toward other cells as intercellular calcium waves (3, 4). Theoretically, intercellular Ca^{2+} signaling may occur through different pathways, namely paracrine or junctional routes. Numerous studies have reported that paracrine and/or junctional routes are involved in the propagation of intercellular calcium waves in a large spectrum of cell types including, for example, astrocytes (5, 6), chondrocytes (7), hepatocytes (8), pancreatic acinar cells (9, 10), or tracheal epithelial cells (11, 12). Most of these studies were performed under particular experimental conditions, i.e., after mechanical stimulation of a single cell from a cultured monolayer, which induces the propagation of Ca^{2+} waves in the connected cells. Such experimental studies on epithelial tracheal ciliated cells, glial cells, and endothelial cells allowed Sneyd et al. (13, 14) to propose a theoretical model accounting for the propagation of intercellular Ca^{2+} waves in these cell types. This model is based on the passive diffusion of inositol 1,4,5-trisphosphate ($InsP_3$) between adjacent cells through gap junctions. $InsP_3$ is produced in the mechanically stimulated cell and provokes the release of Ca^{2+} from internal stores, in the form of an intracellular Ca^{2+} wave propagating via Ca^{2+}-induced Ca^{2+} release (2). Because $InsP_3$ is supposed to move through gap junctions, similar Ca^{2+} waves are initiated in adjacent cells. This phenomenon reproduces itself as long as the amount of $InsP_3$ entering a cell is large enough to induce a Ca^{2+} wave. The model thus accounts for the propagation of a restricted intercellular Ca^{2+} wave after focal stimulation of one individual cell, as well as for asynchronous Ca^{2+} oscillations that occur after the passage of the wave, as often observed in glial cells (14, 15).

In contrast to the studies that led to the model proposed by Sneyd et al. (13), some experiments

[1] Correspondence: Unité de Recherche U442, Institut National de la Santé et de la Recherche Médicale, Université de Paris sud, bâ 443, 91405 Orsay, France. E-mail: laurent.combettes@ibaic.u-psud.fr

have been performed in freshly isolated systems of connected cells that are globally stimulated by hormones, or intact organs perfused with agonists (9, 16–19). Especially in the liver, a striking feature of the responses observed in the latter experimental conditions is the sequential pattern of Ca^{2+} increases in the different coupled cells, creating the appearance of intercellular Ca^{2+} waves. This occurs both in hepatocyte doublets and triplets and in liver cell plates from whole perfused organs. The same sequence of Ca^{2+} responses is observed for each spike for intermediate doses of agonists that cause Ca^{2+} oscillations (17). This sequence of cellular responses to a given agonist is maintained when stimulation is repeated and does not depend on agonist concentration. Thus, interhepatocyte Ca^{2+} waves, although elicited by global agonist stimulation, appear to be oriented in a specific direction in multiplets or in the perfused intact liver (17–19).

Experimental results obtained in multiplets of connected hepatocytes and in the perfused liver suggest that the mechanism for intercellular calcium wave propagation in hepatocytes considerably differs from that in tracheal epithelial cells or endothelial cells. First, in contrast with the latter cell types in which only one Ca^{2+} wave propagates concentrically after focal stimulation, repetitive Ca^{2+} waves propagate in multiplets of hepatocytes (17, 20, 21) or in the intact perfused liver (18, 19). Second, each hepatocyte needs a stimulus (here in the form of an agonist such as vasopressin or norepinephrine) to relay the intercellular Ca^{2+} wave (20). However, gap junction permeability is essential for coordinating Ca^{2+} oscillations in the coupled cells (16, 20). Coordinated intercellular Ca^{2+} signals in connected hepatocytes thus require both effective gap junctions and global hormonal stimulation. Third, a crucial aspect of interhepatocyte Ca^{2+} signals is the spatial orientation of the Ca^{2+} wave, which is unidirectional for a given agonist, as described above. We have suggested that this oriented pattern relies on the observed gradient in hepatocyte sensitivity to agonists along the liver cell plate (21). The appearance of intercellular Ca^{2+} waves could thus arise from the fact that each individual hepatocyte in the liver cell plate (or in multiplets) displays repetitive Ca^{2+} spikes with a slight phase-shift with respect to neighboring cells.

The aim of this study is to develop a theoretical model for the propagation of intercellular Ca^{2+} waves in connected hepatocytes, which could account for this dual control by gap junction permeability and hormonal stimulation. The model is based on the observation that the number of external receptors on the membrane of a hepatocyte depends on its location in the liver cell plate (21). Thus, we assume in the model that a multiplet of connected hepatocytes behaves as a set of individual Ca^{2+} oscillators characterized by slightly different periods, since the period of Ca^{2+} oscillations directly depends on the number of hormonal receptors that have been stimulated (via intracellular $InsP_3$). These oscillators are in turn coupled by an intercellular messenger, which may *a priori* be either Ca^{2+} or $InsP_3$ diffusing through gap junctions. Our results suggest that there is a better agreement between the model and the experimental data when $InsP_3$ is considered as the coordinating messenger. The model based on the hormonal sensitivity gradient and the diffusion of $InsP_3$ through gap junctions leads to theoretical predictions that are confirmed experimentally.

MATERIALS AND METHODS

Materials

Fura 2/AM and Fura 2 were obtained from Molecular Probes, Inc. or Teflab, William's medium E was from Life Technologies, Inc., ionomycin was from Calbiochem, and collagenase was from Boehringer. All other chemicals were purchased from Sigma and were of the highest grade available commercially.

Preparation of hepatocytes

Single hepatocytes and multicellular systems were prepared from fed female Wistar rats by limited collagenase digestion of the liver, as described previously (17). After isolation, rat hepatocytes were maintained (2×10^6 cells/ml) at 4°C in William's medium E supplemented with 10% fetal calf serum, penicillin (200,000 units/ml), and streptomycin (100 mg/ml). Cell viability, assessed by trypan blue exclusion, remained greater than 96% for 4–5 h.

Loading of hepatocytes with Fura 2

Hepatocytes were loaded with Fura 2 either by injection (see below) or by incubation with the dye, as described previously (20). Small aliquots of the suspended hepatocytes (5×10^5 cells) were diluted in 2 ml of William's medium E modified as described above. The cells were then plated onto dish glass coverslips coated with collagen I, and incubated for 60 min at 37°C under an atmosphere containing 5% CO_2. After cell plating, the medium was removed and replaced with a William's medium E containing 3 μM Fura 2/AM. The hepatocytes were then incubated for 30 min at 37°C under an atmosphere containing 5% CO_2. The coverslips were then washed twice with a saline solution (10 mM HEPES, 116 mM NaCl, 5.4 mM KCl, 1.8 mM $CaCl_2$, 0.8 mM $MgCl_2$, 0.96 mM NaH_2PO_4, 5 mM $NaHCO_3$, and 1 g/l glucose, pH 7.4). An Eppendorf microinjector (5242) was used to microinject Fura 2 as described previously (20). After microinjection, cells were allowed to recover for at least 10 min. The success of microinjection was assessed by monitoring the morphology of cells before and after manipulation and checking the ability of the cell to retain injected Fura 2 and low $[Ca^{2+}]_i$. Freshly isolated doublets and triplets were distinguished from aggregates of non-connected cells in conventional light microscopy

by screening for dilated bile canaliculi, which are indicators of maintained functional polarity (22).

Determination of $[Ca^{2+}]_i$ changes in hepatocytes

Dish coverslips were put onto a thermostated holder (34°C) on the stage of a Zeiss Axiovert 35 microscope set up for epifluorescence microscopy. The excitation light was supplied by a high-pressure xenon arc lamp (75 W), and the excitation wavelengths were selected by 340 and 380 nm filters (10-nm bandwidth) mounted in a processor-controlled rotating filter wheel (Sutter) between the ultraviolet lamp and the microscope. Ca^{2+} imaging was performed as described by Combettes et al. (17). Briefly, fluorescence images were collected by a low-light-level ISIT camera (Lhesa, France), digitized, and integrated in real time by an image processor (Metafluor, Princeton, NJ).

Superfusion

Cells were continuously superfused with control or test solutions (at 34°C) by six inlet tubes converging on the coverslip chamber. The perfusion rate was 1.5 to 2 ml/min and the chamber volume was ~0.2 ml. The medium was continuously renewed by aspiration. Agonists were rapidly removed during the Ca^{2+} response with this superfusion system, by increasing the perfusion rate to 4 ml/min to improve the washing efficiency.

Microperfusion

As described previously (20), agents were applied locally by positioning a micropipette (Femtotips, Eppendorf) close to the cell of interest and applying a constant pressure (120 hPa) via the Eppendorf injector. This allowed the delivery of picoliter quantities of agonist-containing solution. To monitor the extent of microperfusion, fluorescein (30 μM) was included in the micropipette and the fluorescein image was monitored at 510 nm using an excitation wavelength of 480 nm.

DESCRIPTION OF THE MODEL

Model for intracellular Ca^{2+} oscillations and waves

In this study, the intracellular Ca^{2+} dynamics of each hepatocyte are described by a model based on sequential activation-deactivation of the $InsP_3$ receptor/Ca^{2+} channel ($InsP_3R$) (23, 24). It is assumed that $InsP_3$- and Ca^{2+}-mediated activation are instantaneous, whereas Ca^{2+}-induced inactivation develops slowly; if activation and inhibition are considered as cooperative processes, the change in the fraction of inactive $InsP_3$ receptors (R_{des}) obeys the following equation (see references for a detailed description of the equations):

$$\frac{dR_{des}}{dt} = k_+ C_{cyto}^{n_i} \frac{1 - R_{des}}{1 + \left(\frac{C_{cyto}}{K_{act}}\right)^{n_a}} - k_- R_{des} \qquad (1)$$

where k^+ and k^- are the kinetic constants of Ca^{2+} association to and dissociation from the inhibitory Ca^{2+} binding site of the $InsP_3R$, C_{cyto} represents the concentration of cytosolic Ca^{2+}, and K_{act} is the dissociation constant of Ca^{2+} binding to the activating Ca^{2+} binding site of the $InsP_3R$. The time evolution of the concentration of cytosolic Ca^{2+} is given by:

$$\frac{dC_{cyto}}{dt} = k_1(b + IR_a)[Ca_{tot} - C_{cyto}(\alpha + 1)] - V_{MP} \frac{C_{cyto}^{n_P}}{C_{cyto}^{n_P} + K_P^{n_P}} \qquad (2)$$

in which IR_a represents the fraction of active (i.e., open) $InsP_3R$ and is given by:

$$IR_a = IR_{able} \frac{1}{1 + \left(\frac{K_{act}}{C_{cyto}}\right)^{n_a}}$$

where IR_{able} is the fraction of receptors that can be activated,

$$IR_{able} = (1 - R_{des}) \frac{Ip^{n_R}}{K_{IP}^{n_R} + Ip^{n_R}}$$

and Ip is the intracellular concentration of $InsP_3$. k_1 is the kinetic constant governing the flux of Ca^{2+} from the lumen into the cytosol and $k_1 b$ is the basal efflux in the absence of $InsP_3$. K_{Ip} is the dissociation constant of $InsP_3$ binding to its receptor. In agreement with experimental results, activation of the $InsP_3R$ by $InsP_3$ is taken as a cooperative process, with a Hill coefficient n_R (25, 26). Ca_{tot} represents the total intracellular Ca^{2+} concentration. If C_{lum} represents the intraluminal Ca^{2+} concentration, $Ca_{tot} = C_{lum} + \alpha C_{cyto}$ where α is the ratio between the volume of the $InsP_3$-sensitive Ca^{2+} pool and the volume of the cytosol. No equation explicitly describes the change in the intraluminal Ca^{2+} concentration (C_{lum}) over time, as the total intracellular Ca^{2+} concentration remains constant and equal to Ca_{tot}. Note that this assumption does not hold if it is assumed that Ca^{2+} diffuses through gap junctions, in which case another equation for the change in C_{lum} needs to be considered. As shown previously (24), the model defined by *Eqs. 1* and *2* accounts for intracellular Ca^{2+} oscillations resembling those observed experimentally. By incorporating diffusion of cytosolic Ca^{2+} in *Eq. 2*, the model also accounts for the propagation of intracellular Ca^{2+} waves. Here, we focus on multiplets of connected hepatocytes (doublets or triplets), which allows us to look at our system in one dimension.

It should be pointed out, however, that our results describing a possible mechanism for intercellular Ca^{2+} wave propagation do not depend on the precise model used to describe the intracellular Ca^{2+} dynamics. We have verified that the outcome remains qualitatively unchanged when the intracellular Ca^{2+} dynamics are described by the model developed by Atri et al. (27), instead of *Eqs. 1* and *2* above. Other models for intracellular Ca^{2+} oscillations and waves, also involving the stimulation of the $InsP_3R$ activity by Ca^{2+}, could also have been used (28–30). Moreover, we neglect any possible spatial inhomogeneity in the intracellular distribution of $InsP_3$ receptors because the main rate-limiting processes are related to $InsP_3$ synthesis, degradation, and passage through gap junctions; the characteristic time for $InsP_3$ diffusion through a hepatocyte is indeed on the order of 100 ms, whereas the characteristic times for the other processes are at least on the order of a few seconds.

In view of the fact that in the model $InsP_3$ can diffuse through gap junctions (**Fig. 1**), its progression over time needs to be considered in the description of the Ca^{2+} dynamics in each individual cell. To this end, we have incorporated in the model a general equation describing synthesis of $InsP_3$ by phospholipase C (PLC) and $InsP_3$ metabolism by $InsP_3$ 3-kinase and 5-phosphatase (see ref. 31). The change in $InsP_3$ over time is therefore determined by:

$$\frac{dIP}{dt} = V_{PLC} - V_K \frac{Ip}{K_K + Ip} \frac{C_{cyto}^{n_d}}{K_d^{n_d} + C_{cyto}^{n_d}} - V_{PH} \frac{Ip}{K_{PH} + Ip} \qquad (3)$$

where V_{PLC} is the velocity of $InsP_3$ synthesis by PLC, which depends on the level of stimulation. V_K and V_{PH} are the maximal velocities of $InsP_3$ metabolism by 3-kinase and 5-phosphatase, respectively, and K_K and K_{PH} are the Michaelis constants characterizing the latter enzymes. In *Eq. 3*, the rate of $InsP_3$ synthesis is assumed to be independent of the level of cytosolic Ca^{2+} (32, 33). Stimulation of $InsP_3$ 3-kinase activity by Ca^{2+} (in reality through Ca^{2+}/calmodulin) is reflected in *Eq. 3* by K_d, which is the threshold constant for activation, and n_d, the Hill coefficient characterizing the latter process. In fact, as emphasized in a previous study (31), $InsP_3$ metabolism is dominated by $InsP_3$ 5-phosphatase. In the model, oscillations of $InsP_3$ due to the stimulation of 3-kinase activity by Ca^{2+} are negligible.

As previously reported (34), in the simulations of the model defined by *Eqs. 1–3*, the latency (that is, the time interval between the onset of stimulation and the peak of the first Ca^{2+} spike) directly depends on the rate of $InsP_3$ synthesis, V_{PLC}. The first Ca^{2+} spike indeed occurs when the concentration of $InsP_3$ reaches a threshold value. Thus, to approximately match the theoretical latencies with experimental observations, we have chosen parameter values characterizing $InsP_3$ synthesis and metabolism such as to get a half-time for an increase in $InsP_3$ of ~45 s at low levels of stimulation which, in the model, leads to a latency of ~70 s.

TABLE 1. *List of parameter values*

Parameter	Value
n_i	4
n_a	3
k^+	25 $s^{-1}\mu M^{-4}$
k^-	2.5 10^{-3} s^{-1}
K_{act}	0.34 μM
k_1	42 $\mu M^{-1}s^{-1}$
b	10^{-4}
V_{MP}	8 μM/s
K_P	0.4 μM
n_P	2
α	0.1
Ca_{tot}	60 μM
K_{IP}	1 μM
V_K	7.5 10^{-3} μM/s
V_{PH}	7.5 10^{-2} μM/s
K_K	1 μM
K_{PH}	10 μM
K_d	0.5 μM
n_d	2
D_{IP}	210 $\mu m^2/s$
D_{Ca}	30 $\mu m^2/s$

Incorporation of gap junctions

In the liver or in freshly isolated multicellular systems of rat hepatocytes, cells are tightly coupled by gap junctions (35). The latter allow the diffusion of diverse small-sized molecules between adjacent cells. We have attempted to incorporate $InsP_3$ diffusion through gap junctions in our model. If Ca^{2+} was the messenger, the same equation would hold after changing Ip into C_{cyto} (see below). Thus, in the model we assume that at each cell boundary the flux is dependent on both the concentration difference across the membrane and on the permeability of the gap junction to $InsP_3$. We have therefore used the same mathematical formulation as Sneyd et al. (14). At each boundary between two cells:

$$D_{IP}\frac{\partial IP^-}{\partial x} = D_{IP}\frac{\partial IP^+}{\partial x} = F_{IP}(IP^+ - IP^-) \qquad (4)$$

where the superscripts + and - indicate the $InsP_3$ concentration at the right and left limits of the border, respectively. The spatial coordinate is indicated by x. The intracellular diffusion coefficient for $InsP_3$ is represented by D_{Ip}. The junctional permeability to $InsP_3$, F_{IP}, is an unknown parameter whose value was chosen such as to best mimic experimental observations. If $F_{IP} = 0$, no $InsP_3$ can diffuse between adjacent cells, and *Eq. 4* reduces to no flux boundary conditions; infinitely large values for F_{IP} correspond to the absence of any cell membrane (Fig. 1).

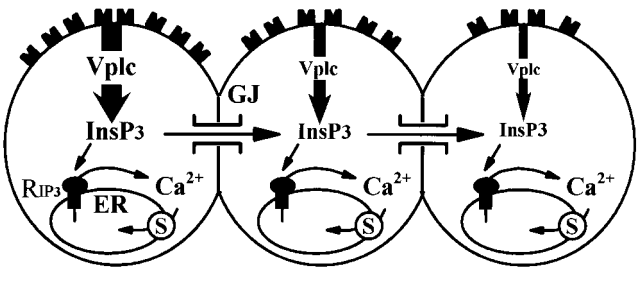

Figure 1. Schematic diagram of the receptor-oriented and coordinated intercellular Ca^{2+} waves in rat hepatocytes. ER, endoplasmic reticulum; S, SERCA; Vplc, velocity of $InsP_3$ synthesis by PLC; GJ, gap junction; RIP_3, IP_3 receptor-Ca^{2+} channel.

The model *Eqs. 1–4* were solved by the finite difference method on an array of two or three cells, each containing 20 grid points. Each cell was assumed to be 20 μm long. Integration was performed numerically using a fourth-order, variable time-step Runge-Kutta method. Parameter values are listed in **Table 1**, except for the rate of $InsP_3$ synthesis (V_{PLC}) and the junctional permeability to $InsP_3$ (F_{IP}), whose value is discussed below.

Gradient of hormonal sensitivity among connected hepatocytes

It is well known that hepatocytes contribute differently to a large number of biological processes depending on their location in the portocentrilobular axis of the liver acinus (36). In the same manner, there is morphological evidence for a gradient of vasopressin receptors along the liver cell plate (18, 37). This increasing density of hormonal receptors from the periportal to the perivenous zones of the liver cell plate may account for a gradient of sensitivity to vasopressin that we have observed recently (21). Indirect evidence suggesting the existence of a similar gradient for α-adrenoceptors has been reported previously (21, 38). In this experiment, global perfusion of norepinephrine elicited a sequential Ca^{2+} response in a hepatocyte triplet (**Fig. 2**, left). When the agonist was quickly removed from the medium, immediately after Ca^{2+} levels increased in the second cell, the third cell did not respond (Fig. 2, middle). Similarly, when the agonist was removed by rapidly washing the medium immediately after Ca^{2+} levels increased in the first cell, the second and the third cells did not respond (Fig. 2, right). Thus, in conditions where cells are uniformly perfused with norepinephrine, the time of contact between the agonist and the cell necessary to induce a Ca^{2+} response is largest in the last and shortest in the first responding hepatocyte. This experiment thus argues for a gradual change in hepatocyte sensitivity to norepinephrine in multiplets.

Such sensitivity gradients are taken into account in the

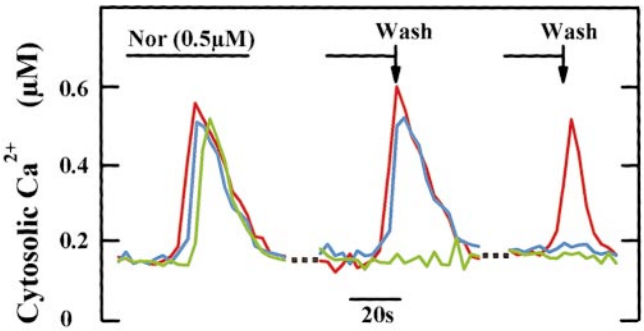

Figure 2. Sensitivity gradient to norepinephrine. Hepatocytes injected with Fura 2 were challenged with norepinephrine (Nor, 0.5 μM) for the time shown by the horizontal bar. The solution was rapidly washed out as indicated by the arrow. After norepinephrine addition to the bath, intercellular Ca^{2+} waves initiated in cell 1 (red) propagate to cells 2 (blue) and 3 (green). After washout of norepinephrine at the peak of the $[Ca^{2+}]_i$ increase in cell 2 (middle) or cell 1 (right), there was no further propagation to associated cells (respectively, cell 3 or 3 and 2). These results are representative of those obtained using 4 triplets in 3 independent experiments.

model (illustrated in Fig. 1) by assuming that each cell has a different velocity of $InsP_3$ synthesis by phospholipase C (V_{PLC}). It has been estimated that the mean number of V1a vasopressin binding sites in the perivenous zone of the cell plate exceeds by 40% the mean number of the same binding sites in the periportal zone (21). Thus, assuming that the average number of cells in a cell plate is ~20, then the model presumes that V_{PLC} differs by 5% between two neighboring hepatocytes. In the model, for the parameter values listed in Table 1, a 5% difference in V_{PLC} leads to variations of ~20% in the period of Ca^{2+} oscillations.

Cellular heterogeneity is clearly dominated by these variations in the rate of $InsP_3$ synthesis; indeed, when caged $InsP_3$ is microinjected into one cell of Fluo3-loaded doublets and triplets of hepatocytes, the Ca^{2+} increases observed after flash photolysis appear to be nearly identical and simultaneous in the connected cells (21). This strongly suggests that the behavior of distinct hepatocytes, which were originally closely located in the cell plate, is nearly identical when the steps responsible for $InsP_3$ synthesis are bypassed.

RESULTS AND DISCUSSION

Estimation of the permeability of gap junctions

Several studies have suggested that the propagation of an intercellular hepatic Ca^{2+} wave requires junctional connectivity (18, 19), mainly because the microinjection of large amounts of Ca^{2+} or $InsP_3$ in one cell of a doublet increases Ca^{2+} in the connected cell (39). It has also been reported that gap junctional permeability is essential for coordination of Ca^{2+} signaling in coupled hepatocytes (16, 20). However, little is known about the extent of $InsP_3$ intercellular diffusion during agonist stimulation. We have shown recently that when one cell within a doublet is stimulated by submaximal doses of norepinephrine, the amount of messenger diffusing through the gap junctions is insufficient on its own to induce a Ca^{2+} response in the adjacent cell (20). Similarly, as shown in **Fig. 3*A***, focal vasopressin stimulation of a single cell in a doublet induces Ca^{2+} oscillations that are limited to the stimulated hepatocyte and do not show up in the connected cell. At the end of the experiment, when the doublet is globally superfused with vasopressin (0.1 nM), both cells exhibit Ca^{2+} oscillations that are sequential and well coordinated (Fig. 3*B*).

We have used this experiment to evaluate the permeability coefficient (F_{IP}), to be incorporated in the model. To this end, we considered a theoretical doublet, consisting of two Ca^{2+} oscillators whose values for V_{PLC}, the parameter reflecting the rate of $InsP_3$ synthesis, differ by 5%. We then performed

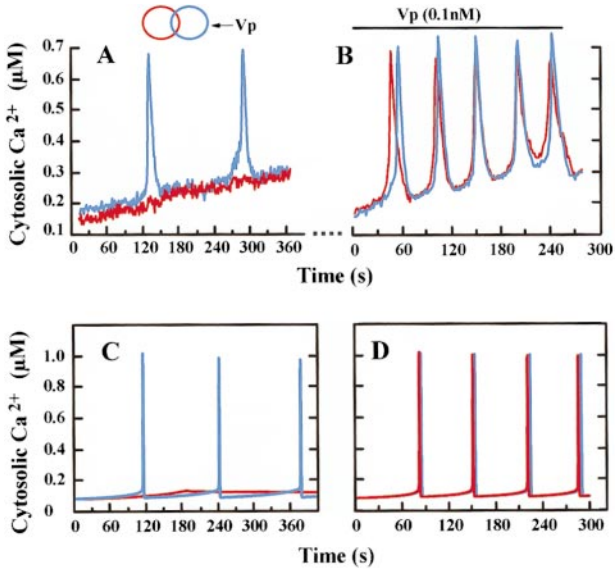

Figure 3. Focal stimulation of connected rat hepatocytes. *A, B*) Hepatocytes were loaded or injected with Fura 2. Successive measures of $[Ca^{2+}]_i$ in the same hepatocyte doublet are shown. One cell within the doublet was focally microperfused with vasopressin (Vp; 10 μM in the micropipette), as described in Materials and Methods. Only the stimulated cell (indicated by arrow) within the doublet responded (*A*). The micropipette was then removed and the cell preparation was washed. After 5 min, the doublet was globally superfused with vasopressin (0.1 nM) for the time shown by the horizontal bars. Both cells of the doublet exhibited tightly coordinated $[Ca^{2+}]_i$ oscillations (*B*). Tracings were interrupted during the washing process (the gap represents 4 min). *C, D*) Numerical simulations of the experiments shown above. A value of 0.88 μm/s for the $InsP_3$ permeability coefficient (F_{IP}) allows the model to reproduce the experimental results shown above. If only one cell is assumed to be stimulated (C), it fails to induce Ca^{2+} spikes in the connected, unstimulated cell. In contrast, when both cells are stimulated, coordinated Ca^{2+} spiking is observed (*D*). Results were obtained by numerical integration of the model defined by *Eqs. 1–4* with parameter values listed in Table 1, with $V_{PLC} = 6.5 \times 10^{-4}$ μM/s (red line) and 2.77×10^{-3} μM/s (blue line) for *panel C*, and $V_{PLC} = 2.205 \times 10^{-3}$ μM/s (red line) and 2.1×10^{-3} μM/s (blue line) for *panel D*. Initial conditions are resting states corresponding to $V_{PLC} = 6.5 \times 10^{-4}$ μM/s.

successive trials to determine a value for F_{IP} that allows for both coordination of Ca^{2+} spiking when the whole doublet is stimulated (lower limit for F_{IP}), and for the absence of Ca^{2+} variations in an unstimulated cell connected to an oscillating one (upper limit for F_{IP}). In Fig. 3*C, D*, each color represents the change in Ca^{2+} concentration in a given cell. For a value of the permeability coefficient (F_{IP}) equal to 0.88 μm/s, Ca^{2+} oscillations were restricted to the stimulated cell (in blue), as shown in Fig. 3*C*; on global stimulation both cells oscillated, with a slight phase-shift (Fig. 3*D*). A similar result was obtained for other F_{IP} values differing by ~10%. This value for the permeability coefficient F_{IP}, which is close to the one predicted in previous theoretical studies (13, 14, 40), was thus used for the remaining simulations.

Phase waves of Ca^{2+} increases among connected hepatocytes

We have simulated the behavior of three hepatocytes whose values for V_{PLC} differ by 5%. These cells were assumed to be connected by gap junctions allowing the diffusion of $InsP_3$, by considering the boundary conditions given in *Eq. 4* and the permeability coefficient estimated above. As shown in **Fig. 4*A***, the Ca^{2+} oscillations generated by the model were tightly coordinated among the three cells. The change in cytosolic Ca^{2+} in the most sensitive cell, i.e., the one with the largest value for V_{PLC}, is shown in red; less-sensitive cells are shown in blue and green, respectively. As previously observed experimentally (17, 21), peaks of cytosolic Ca^{2+} appeared sequentially in cells 1 (red), 2 (blue), and 3 (green), giving the appearance of an intercellular Ca^{2+} wave. Because we assumed in the model that no Ca^{2+} is transported from one cell to another, this wave is in fact a "phase wave" (41). This means that the appearance of a wave propagation phenomenon comes from the slight phase-shift between the individual oscillators. This phase-shift originates because the three cells of the triplet do not simultaneously enter into the oscillatory domain because of their different values for V_{PLC}.

Variations in V_{PLC} also cause the period of Ca^{2+} oscillations to be different in the three cells, resulting in a progressive loss of coordination. Figs. 3*D* and 4*A* show that, in the model, the delay between Ca^{2+} spiking in adjacent cells increased with time. Thus, the model predicts that after a sufficient number of apparent intercellular Ca^{2+} waves the hepatocytes will oscillate in a less synchronous manner. This is because in each cell the frequency of Ca^{2+} oscillations is imposed by the level of $InsP_3$, whose value depends on both hormonal sensitivity (V_{PLC}) and diffusion through gap junctions (F_{IP}). The delay between Ca^{2+} spiking, and thus the velocity of the apparent intercellular Ca^{2+} wave, is then fixed by these differences in the levels of $InsP_3$, which themselves depend on the parameters affecting synthesis, metabolism, and diffusion of this messenger. In particular, as expected intuitively, coordination was enhanced when the permeability coefficient was increased or when the sensitivity gradient was decreased (data not shown). Also, coordination increased with the level of stimulation, a property that is reflected by the fact that the velocity of the intercellular Ca^{2+} wave rises with agonist concentration, as shown in the experiments (17–19).

That the level of synchronization is better for the first few spikes after stimulation is indeed experi-

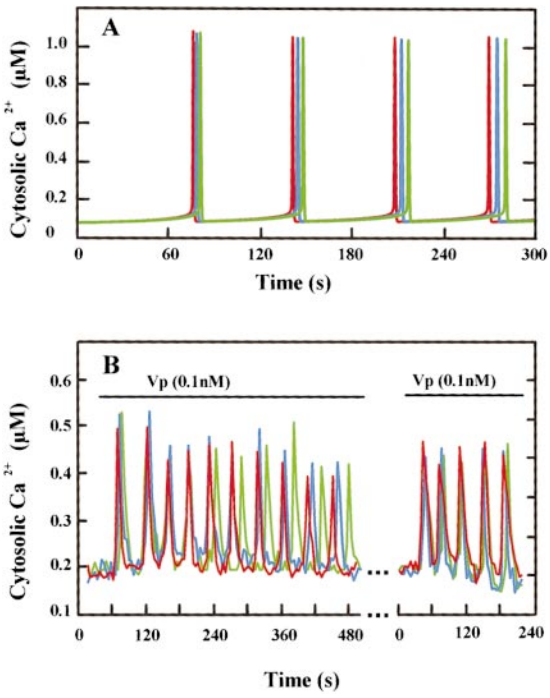

Figure 4. Ca^{2+} oscillations and intercellular Ca^{2+} waves induced by vasopressin in a triplet of hepatocytes. *A*) Numerical simulation of the Ca^{2+} response in three cells differing in their sensitivity to the agonist, i.e., in their values for parameter V_{PLC}. Spikes appear in a sequential manner, giving the appearance of intercellular Ca^{2+} waves. However, coordination is progressively lost because the three cells have different stationary levels of $InsP_3$. Results were obtained by numerical integration of the model defined by *Eqs. 1–4* with parameter values listed in Table 1, with $V_{PLC} = 2.3 \times 10^{-3}$ μM/s (red line), 2.2×10^{-3} μM/s (blue line), and 2.1×10^{-3} μM/s (green line). Initial conditions are resting states corresponding to $V_{PLC} = 6.5 \times 10^{-4}$ μM/s. The permeability coefficient for $InsP_3$ (F_{IP}) is 0.88 μM/s. B) Hepatocytes loaded with Fura 2 were stimulated with vasopressin (Vp, 0.1 nM) for the time shown by the horizontal bars. Addition of Vp to the bath induced coordinated $[Ca^{2+}]_i$ oscillations in the three cells, which progressively desynchronized (*B, left*). Vp was then removed and cells were extensively washed (5 min). The same concentration of Vp was then re-applied and the three cells rapidly recovered synchronized $[Ca^{2+}]_i$ oscillations (*B, right*). These results are representative of those obtained using 8 triplets in 4 independent experiments. Recording of the traces was interrupted during the washing process (5 min).

mentally observed in most cases; one example is shown in Fig. 4*B*. The loss of coordination among this triplet of connected hepatocytes was not due to a time-dependent alteration of the cells. Indeed, resynchronization could be achieved by washing and restimulation of the same triplet by an identical concentration of vasopressin (Fig. 4*B*, right).

In the model, the gradual loss in coordination can be explained by the fact that the apparent intercellular Ca^{2+} waves are actually the result of uncoupled oscillators because $InsP_3$ does not oscillate significantly during the course of Ca^{2+} oscillations. Thus, initial coordination arises because of the initial conditions and the proximal levels of $InsP_3$ prevailing during the evolution of the three cells toward their steady state situations. However, because the oscillators are basically uncoupled, they do not remain coordinated for long time periods.

On the basis of estimates of the mean numbers of V1a vasopressin binding sites in the perivenous and periportal zones along the liver cell plate, we assumed in the model a well-organized gradient of V_{PLC} within a triplet. This assumption allowed us to mimic experimental observations as well as to make appropriate theoretical predictions (see below). However, if this organization is not respected, e.g., if the least or the most sensitive cell of a triplet is the central one, the model predicted that the coordination of Ca^{2+} oscillations would be maintained, but the appearance of a unidirectional Ca^{2+} wave would be lost (data not shown). Such a coordinated Ca^{2+} response, in which the Ca^{2+} spike first occurs in the intermediate cell, has been reported experimentally (17) and could be the result of the three-dimensional network of liver cell plates that branch and bend back onto themselves (42).

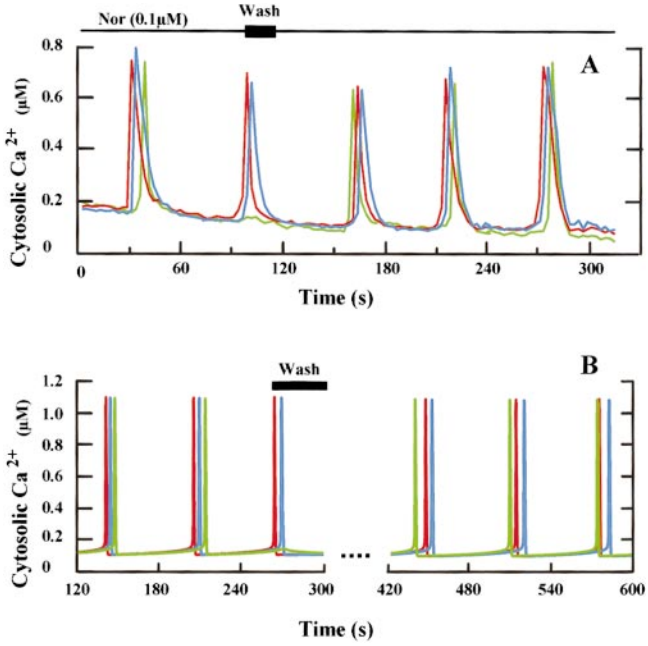

Figure 5. Effect of agonist removal during synchronized Ca^{2+} oscillations. *A*) Results were obtained as in Fig. 1. Hepatocytes loaded with Fura 2 were stimulated with norepinephrine (Nor, 0.1 μM) for the time shown by the horizontal bar. The solution was rapidly washed out (W), as indicated by the black rectangle. These results are representative of those obtained using 5 triplets in 4 independent experiments. *B*) Simulations of the experiment shown in *panel A*. Washing is simulated by an instantaneous return of V_{PLC} to its basal level just after the appearance of a Ca^{2+} spike in the intermediate cell. When the washing time is short, the cell that had failed to respond spikes first after the readdition of the agonist (*B*, green line). Results have been obtained as in Fig. 3*A*, except that V_{PLC} is set at the resting value (6.5×10^{-4} μM/s) between $t = 275$ s and $t = 375$ s (*B*), as indicated by the horizontal bars.

Theoretical predictions

A peculiar feature of intercellular Ca^{2+} waves in hepatocytes, compared with other cell types, is that they require the continuous presence of an agonist (20). Thus, we compared the results of the model with that of the real cells when the agonist is removed. In **Fig. 5*A***, norepinephrine was used to stimulate a triplet and then, during oscillations, the agonist was rapidly washed out. Spiking did not occur in cell 3 after washing, probably because the level of $InsP_3$ in this cell was too low due to the absence of the agonist. Simulation of this experiment, with the same parameter values as in Figs. 3 and 4, is shown in Fig. 5*B*. A sudden decrease of V_{PLC} to its basal value in the three connected cells (at $t =$ 275 s) prevented Ca^{2+} spiking in cell 3. When V_{PLC} was returned to its stimulated value in all three cells, coordinated Ca^{2+} spiking recovered, similar to that observed in the experiments (Fig. 5*B*). However, in contrast to the situation before washing, cell 3 (green line) spiked first after the agonist was reapplied. This was due to the fact that the fraction of activable $InsP_3$ receptors was slightly higher in this cell because the levels of $InsP_3$ and Ca^{2+} were already raised before washing (see Fig. 5*B*).

Experimentally, such an inversion in the sequence of responses was also observed. Fig. 5*A* shows that when the washing time was short (see below), the initial sequence (cell 1, 2, then 3) was modified (cell 3, 1, then 2). In the model, the initial sequence (cell 1 to 3) recovered after five coordinated spikes, whereas in the experiments, recovery generally occurred sooner (see Fig. 5*A*). A straightforward prediction of the model is that when the time interval during which no $InsP_3$ synthesis occurs (i.e., the washing time) becomes very large, the sequence of Ca^{2+} spikes occurring in response to the second addition of the hormone will be imposed by the hormonal sensitivity, as it is for the first addition of agonist (data not shown). This prediction is in good qualitative agreement with the experimental results, although the time scales do not match the experi-

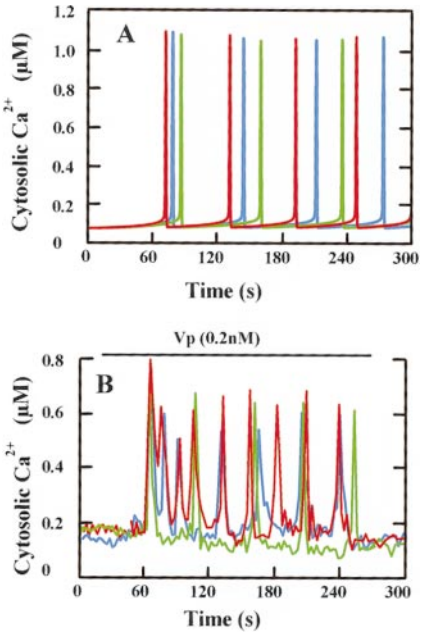

Figure 6. Ca^{2+} oscillations in AGA-treated hepatocytes in response to stimulation by vasopressin. *A*) Simulation of the Ca^{2+} increase in three uncoupled cells ($F_{IP} = 0$) differing by their V_{PLC} values. The first Ca^{2+} spike appears in a more or less coordinated manner, although subsequent spikes occur independently in the different cells. Results have been obtained as in Fig. 4*A*, except that F_{IP} is equal to 0. B) Hepatocytes loaded with Fura 2 were incubated with AGA (20 μM) for 20 min. Then, vasopressin (Vp, 0.2 nM) was added for the time shown by the horizontal bar in presence of AGA. These results are representative of those obtained using 4 triplets (and 7 doublets) in 3 independent experiments.

mental observations (i.e., the washing time needs to be longer in the model than in reality). Analysis of 12 multiplets of connected hepatocytes (7 doublets and 5 triplets) showed that when the washing time was greater than 50 s, no inversion was observed. In contrast, the cell that had been prevented from responding was the first responding cell after washing when the washing time was below 30 s.

Experimental observations have clearly shown that effective gap junctions are necessary to coordinate Ca^{2+} spiking in connected hepatocytes. In the model, gap junctions reduced the differences in the levels of $InsP_3$ because of the imposed gradient in the rates of $InsP_3$ synthesis (V_{PLC}). Because the gradient in hormonal sensitivity is tenuous (a value of 5% between two adjacent cells is used in the simulations), it is expected that some level of coordination in Ca^{2+} spiking should be observed in neighboring cells, even if the cells are not connected through gap junctions. This point is illustrated by the results shown in **Fig. 6*A***; this simulation was performed under the same conditions as Fig. 4*A*, except that the permeability of the gap junctions to $InsP_3$ (F_{IP}) was set to zero. It is clearly visible that the first Ca^{2+} spike is coordinated in the three cells. This is due to the fact that, after the rise in $InsP_3$ resulting from the increase in V_{PLC}, the three cells enter the oscillatory domain at about the same time. However, because the stationary values of $InsP_3$ concentrations are significantly different, each cell oscillates afterward at its own frequency and spiking occurs independently in the different cells. This mechanism bears much similarity with that proposed by Jafri and Keizer to account for intracellular Ca^{2+} waves in *Xenopus* oocytes (43).

This property of the model is corroborated by the experiment shown in Fig. 6*B*. The first Ca^{2+} spike after stimulation of a triplet of hepatocytes pretreated with AGA, a gap junction inhibitor, occurred nearly at the same time in all three cells, although thereafter there was no coordination of Ca^{2+} spiking among the three cells. Then, if it is possible in principle to coordinate the first few Ca^{2+} spikes in

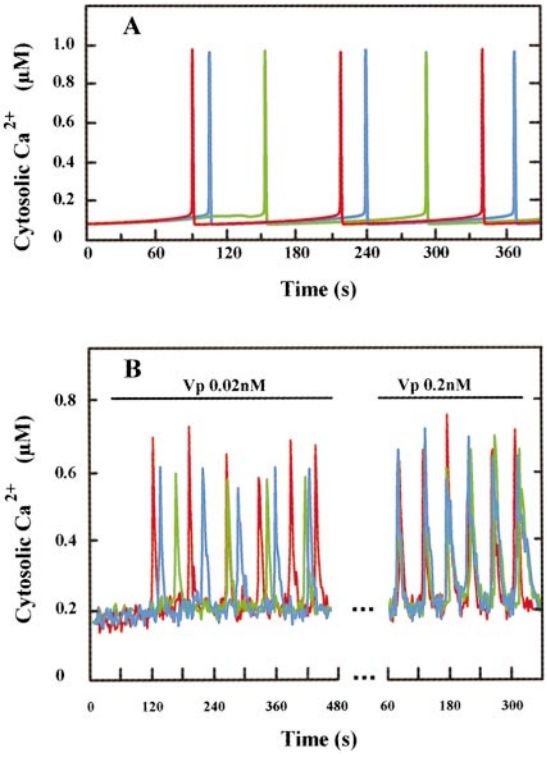

Figure 7. Absence of coordination among the Ca^{2+} spikes in connected hepatocytes at low stimulation levels. *A*) Simulation of Ca^{2+} spikes in a triplet of connected hepatocytes in response to a low level of stimulation, i.e., $V_{PLC} = 1.9 \times 10^{-3}$ μM/s (red), $V_{PLC} = 1.8 \times 10^{-3}$ μM/s (blue), and $V_{PLC} = 1.7 \times 10^{-3}$ μM/s (green). The cells responded in an asynchronous manner because the relative differences in the levels of $InsP_3$ are important. Except for the values of V_{PLC}, results were obtained as in Fig. 4*A*. *B*) Left and right, successive measurements of $[Ca^{2+}]_i$ in the same hepatocyte triplet loaded with Fura 2. In the left part, vasopressin (Vp, 0.02 nM) addition to the bath was followed by oscillations in the three cells, which were not coordinated. However, after washing (5 min), addition of vasopressin (Vp, 0.2 nM) induced well-coordinated oscillations among the three connected hepatocytes (right). These results are representative of those obtained using 8 triplets in 5 independent experiments.

the absence of gap junctions, e.g., by adjusting the values of some parameters of the model such as the intensity of the gradient in hormonal sensitivity, this mechanism would not be in agreement with the experimental observation that Ca^{2+} spikes are not coordinated if a triplet of cells is treated with gap junction inhibitors (Fig. 6*B* above, see also Fig. 4 in ref. 20). Thus, if we assume in the model differences in hormonal sensitivities matching reasonably well the experimental observations, one has to incorporate $InsP_3$ diffusion through gap junctions to account for the observed coordination in Ca^{2+} spiking among neighboring cells.

The last prediction presented here pertains to the behavior of connected hepatocytes stimulated by very low doses of agonist. Indeed, in the model coordination of Ca^{2+} spikes relied on close levels of $InsP_3$. If the intensity of stimulation is low, the relative differences between the concentrations of $InsP_3$ among the connected cells are more important, although the gradient in the number of receptors remains the same. As shown in **Fig. 7*A***, in the model, very low levels of stimulation led to noncoordinated spiking among a triplet of connected cells. Similar results were also found experimentally (Fig. 7*B*); the same triplet exhibited no coordination at low agonist levels (0.02 nM vasopressin) and good coordination at higher agonist doses (0.2 nM vasopressin).

Model in which Ca^{2+} is the coordinating messenger

We have also tested the hypothesis that Ca^{2+}, and not $InsP_3$, could diffuse through gap junctions. To this end, we have replaced the boundary conditions given in *Eq. 4* by a similar equation for Ca^{2+}; we have also added an equation for changes in the concentration of luminal Ca^{2+} (C_{lum}), because the total intracellular Ca^{2+} concentration does not remain constant. Because the release of Ca^{2+} through the $InsP_3R$ is stimulated by both Ca^{2+} and $InsP_3$, coordination of Ca^{2+} spikes throughout a group of connected cells could in principle also be achieved in this way. However, it should be kept in mind that Ca^{2+} buffering (here taken into account by using an appropriate Ca^{2+} diffusion coefficient) and extrusion from the cytosol are both very efficient and fast processes. Thus, small amounts of Ca^{2+} diffusing through gap junctions would probably not provoke a rise in cytosolic free Ca^{2+} large enough to activate the $InsP_3Rs$ and induce a Ca^{2+} wave. Although the model does not allow us to exclude the hypothesis that intercellular Ca^{2+} waves in hepatocytes rely on the passage of Ca^{2+} through gap junctions, the following negative results suggest that $InsP_3$ is a more likely candidate for coordination.

First, in this model including Ca^{2+} diffusion through gap junctions, the spikes propagated intercellularly with decreasing amplitudes (data not shown). This behavior is due to the fact that spiking in cells 2 and 3 occurs sooner and with lower levels of $InsP_3$ than Ca^{2+} spikes that occur without Ca^{2+} input from adjacent cells. Thus, the fraction of activable $InsP_3$ receptors at the onset of the spikes is lower and the flux through the $InsP_3$ receptor is of reduced amplitude, which is not observed experimentally.

Second, the results of the agonist removal experiment (see Fig. 5) cannot be accounted for by the model based on Ca^{2+} diffusion through gap junctions. Indeed, in this model, when the agonist is removed just after the Ca^{2+} spike in cell 1, the amount of Ca^{2+} transferred through the gap junctions is sufficient to induce a Ca^{2+} spike in cells 2 and 3, even at the reduced levels of $InsP_3$ generated by the sudden return of V_{PLC} to its basal level. Given that $InsP_3$ synthesis and metabolism are relatively slow (to account for latencies on the order of 1 min, see above), the decrease in the level of $InsP_3$ occurring in a few seconds is quite small; as a consequence the level of $InsP_3$ is still high enough to allow the generation of a Ca^{2+} spike in response to the Ca^{2+} input from the adjacent cell. The model thus predicts that the Ca^{2+} permeability necessary to coordinate Ca^{2+} spikes in hepatocytes, whose periods are intrinsically different due to different hormonal sensitivities, is too high to prevent Ca^{2+} spiking in a connected cell in which the level of $InsP_3$ has been decreasing for a few seconds after washing.

Third, the model based on the diffusion of Ca^{2+} through gap junctions cannot account for the asynchronous spiking observed at low levels of stimulation (see Fig. 7). Because the amplitude of the Ca^{2+} spike does not much depend on the level of $InsP_3$, the amount of Ca^{2+} diffusing through gap junctions remains the same for all values of V_{PLC}. As a consequence, spiking is either coordinated or does not occur at all in the less sensitive cell(s), because the level of $InsP_3$ in these cells is too low.

Altogether, these comparisons between theoretical and experimental results led us to conclude that $InsP_3$ diffusion through gap junctions must play a dominant role in the coordination of Ca^{2+} spikes among connected hepatocytes. However, it is possible that Ca^{2+} can also somewhat diffuse through gap junctions and thereby synchronize the Ca^{2+} responses in adjacent cells exhibiting small random variations in the different processes related to Ca^{2+} handling.

Conclusions

Based on the assumption that connected hepatocytes differ in their sensitivity to an agonist, we have shown

that coordinated Ca^{2+} spiking can be ascribed to the diffusion of small amounts of $InsP_3$ through gap junctions. The direction of the gradient of hormonal receptors determines the direction of the wave, whereas its amplitude determines the propagation velocity.

From a more general and physiological point of view, intercellular Ca^{2+} waves in hepatocytes resemble the propagation of signals in some other tissues. For example, the propagation of the action potential in the cardiac sinoatrial node can indeed be described as a phase wave propagating through large groups of cells whose intrinsic periods are different (44). Although there are noticeable differences in intercellular propagation of signals in hepatocytes and cardiac pacemaker cells, in both cases the coordination of the response among a large group of cells optimizes the operation of the whole organ, and the direction of propagation is determined by a gradual heterogeneity in cellular spiking. The physiological impact of such an organization at the multicellular (or tissue) level may be important for orienting cell-to-cell signals in specific directions, not only in the heart but also in other tissues such as the liver or colon (18, 19, 45). FJ

We thank V. Lowes for her help in editing the manuscript. This study was supported by the Actions de Recherche Concertée Program ARC 94–99 (launched by the Division of Scientific Research, Ministry of Science and Education, French Community of Belgium), a FRSM Grant (no. 3.4607.99) and by a CFB-INSERM exchange program. G.D. is Chercheur Qualifié at the Belgian FNRS. T.T is supported by The Fondation pour la Recherche Medicale.

REFERENCES

1. Nathanson, M. H., and Schlosser, S. F. (1996) Calcium signaling mechanisms in liver in health and disease. *Prog. Liver Dis.* **14,** 1–27
2. Berridge, M. (1997) Elementary and global aspects of calcium signalling. *J. Physiol.* **499,** 291–306
3. Sanderson, M., Charles, A., Boitano, S., and Dirksen, E. (1994) Mechanisms and function of intercellular calcium signaling. *Mol. Cell. Endocrinol.* **98,** 173–187
4. Sanderson, M. (1996) Intercellular waves of communication. *News Physiol. Sci.* **11,** 262–269
5. Charles, A. C., Naus, C. C., Zhu, D., Kidder, G. M., Dirksen, E. R., and Sanderson, M. J. (1992) Intercellular calcium signaling via gap junctions in glioma cells. *J. Cell Biol.* **118,** 195–201
6. Venance, L., Stella, N., Glowinski, J., and Giaume, C. (1997) Mechanism involved in initiation and propagation of receptor-induced intercellular calcium signaling in cultured rat astrocytes. *J. Neurosci.* **17,** 1981–1992
7. D'Andrea, P., and Vittur, F. (1997) Propagation of intercellular Ca^{2+} waves in mechanically stimulated articular chondrocytes. *FEBS Lett.* **400,** 58–64
8. Schlosser, S., Burgstahler, A., and Nathanson, M. (1996) Isolated rat hepatocytes can signal to other hepatocytes and bile duct cells by release of nucleotides. *Proc. Natl. Acad. Sci. USA* **93,** 9948–9953
9. Loessberg-Stauffer, P., Zhao, H., Luby-Phelps, K., Moss, R., Star, R., and Muallem, S. (1993) Gap-junction communication modulates $[Ca^{2+}]_i$ oscillations and enzyme secretion in pancreatic acini. *J. Biol. Chem.* **268,** 19769–19775
10. Yule, D., Stuenkel, E., and Williams, J. (1996) Intercellular calcium waves in rat pancreatic acini: mechanism of transmission. *Am. J. Physiol.* **271,** C1285–C1294
11. Hansen, M., Boitano, S., Dirksen, E. R., and Sanderson, M. J. (1993) Intercellular calcium signaling induced by extracellular adenosine 5′-triphosphate and mechanical stimulation in airway epithelial cells. *J. Cell Sci.* **106,** 995–1004
12. Hansen, M., Boitano, S., Dirksen, E. R., and Sanderson, M. J. (1995) A role for phospholipase C activity but not ryanodine receptors in the initiation and propagation of intercellular calcium waves. *J. Cell Sci.* **106,** 2583–2590
13. Sneyd, J., Wetton, B., Charles, A., and Sanderson, M. (1995) Intercellular calcium waves mediated by diffusion of inositol trisphosphate : a two-dimensional model. *Am. J. Physiol.* **268,** C1537–C1545
14. Sneyd, J., Wilkins, M., Strahonja, A., and Sanderson, M. (1998) Calcium waves and oscillations driven by an intercellular gradient of inositol (1,4,5)-trisphosphate. *Biophys. Chem.* **72,** 101–109
15. Charles, A., Kodali, S., and Tyndale, R. (1996) Intercellular calcium waves in neurons. *Mol. Cell Neurosci.* **7,** 337–353
16. Nathanson, M., and Burgstahler, A. (1992) Coordination of hormone-induced calcium signals in isolated rat hepatocyte couplets. Demonstration with confocal microscopy. *Mol. Biol. Cell* **3,** 113–121
17. Combettes, L., Tran, D., Tordjmann, T., Laurent, M., Berthon, B., and Claret, M. (1994) Sequential activation of hormone-mediated Ca^{2+} signals in multicellular systems of rat hepatocytes. *Biochem. J.* **304,** 585–594
18. Nathanson, M., Burgstahler, A., Mennone, A., Fallon, M., Gonzalez, C., and Saez, J. (1995) Ca^{2+} waves are organized among hepatocytes in the intact organ. *Am. J. Physiol.* **32,** G167–G171
19. Robb-Gaspers, L., and Thomas, A. (1995) Coordination of Ca^{2+} signaling by intercellular propagation of Ca^{2+} waves in the intact liver. *J. Biol. Chem.* **270,** 8102–8107
20. Tordjmann, T., Berthon, B., Claret, M., and Combettes, L. (1997) Coordinated intercellular calcium waves induced by noradrenaline in rat hepatocytes: dual control by gap junctions and agonist. *EMBO J.* **16,** 5398–5407
21. Tordjmann, T., Berthon, B., Jaquemin, E., Clair, C., Stelly, N., Guillon, G., Claret, M., and Combettes, L. (1998) Receptor-oriented intercellular calcium waves mediated by a gradient in sensitivity to vasopressin in rat hepatocytes. *EMBO J.* **17,** 4695–4703
22. Gautam, A., Oi-Cheng, N. G., and Boyer, J. L. (1987) Isolated rat hepatocyte couplets in short-term culture: structural characteristics and plasma membrane reorganisation. *Hepatology* **7,** 216–223
23. Swillens, S., Combettes, L., Champeil, P. (1994) Transient inositol 1,4,5-trisphosphate-induced Ca^{2+} release: a model based on regulatory Ca^{2+} binding sites along the permeation pathway. *Proc. Natl. Acad. Sci. USA* **91,** 10074–10078
24. Dupont, G., and Swillens, S. (1996) Quantal release, incremental detection and long-period Ca^{2+} oscillations in a model based on regulatory Ca^{2+} binding sites along the permeation pathway. *Biophys. J.* **71,** 1714–1722
25. Meyer, T., Holowka, D., and Stryer, L. (1988) Highly cooperative opening of calcium channels by inositol 1,4,5-trisphosphate. *Science* **240,** 653–656
26. Dufour, J., Arias, I., and Turner, T. (1997) Inositol 1,4,5-trisphosphate and calcium regulate the calcium channel function of the hepatic inositol 1,4,5-trisphosphate receptor. *J. Biol. Chem.* **272,** 2675–2681
27. Atri, A., Amundson, J., Clapham, D., and Sneyd, J. (1993) A single-pool model for intracellular Ca^{2+} oscillations and waves in the *Xenopus laevis* oocyte. *Biophys. J.* **65,** 1727–1739
28. De Young, G., and Keizer, J. (1992) A single pool inositol 1,4,5-trisphosphate-receptor-based model for agonist-stimulated oscillations in Ca^{2+} concentration. *Proc. Natl. Acad. Sci. USA* **89,** 9895–9899
29. Goldbeter, A. (1996) *Biochemical Oscillations and Cellular Rythms.* Cambridge University Press, Cambridge, UK.
30. Tang, Y., Stephenson, J., and Othmer, H. (1996) Simplification and analysis of models of calcium dynamics based on IP_3-sensitive Ca^{2+} channel kinetics. *Biophys. J.* **70,** 246–263

31. Dupont, G., and Erneux, C. (1997) Simulations of the effects of inositol 1,4,5-trisphosphate 3-kinase and 5-phosphatase on Ca^{2+} oscillations. *Cell Calcium* **22,** 321–331
32. Renard, D., Poggioli, J., Berthon, B., and Claret, M. (1987) How far does phospholipase C activity depend on the cell calcium concentration? *Biochem. J.* **243,** 391–398
33. Bird, G. S., Obie, J. F., and Putney, J. W. (1997) Effect of cytoplasmic Ca^{2+} on (1,4,5)IP3 formation in vasopressin-activated hepatocytes. *Cell Calcium* **21,** 253–256
34. Thomas, A. P., Bird, G. S., Hajnoczky, G., Robb-Gaspers, L. D., and Putney, J. W. (1996) Spatial and temporal aspects of cellular calcium signaling. *FASEB J.* **10,** 1505–1517
35. Spray, D. C., Saez, J. C., Hertzberg, E. L., and Dermietzel, R. (1994) Gap junctions in liver. In: *The liver: Biology and Pathobiology* (Arias, I. M., Boyer, J. L. Fausto, N., Jokoby, W. B., Schachter, D. A., and Shafritz, D. A. eds.) pp. 951–967, Raven Press, New York
36. Jungermann, K., and Kietzmann, T. (1996) Zonation of parenchymal and non parenchymal metabolism in liver. *Annu. Rev. Nutr.* **16,** 179–203
37. Ostrowski, N. L., Young, W. S., Knepper, M. A., and Lolait, S. J. (1993) Expression of vasopressin V1a and V2 receptor messenger ribonucleic acid in the liver and kidney of embryonic, developing, and adult rats. *Endocrinology* **133,** 1849–1859
38. Tordjmann, T., Berthon, B., Combettes, L., and Claret, M. (1996) The location of hepatocytes in the rat liver acinus determines their sensitivity to calcium-mobilizing hormones. *Gastroenterology* **111,** 1343–1352
39. Saez, J., Connor, J., Spray, D., and Bennett, M. (1989) Hepatocyte gap junctions are permeable to the second messenger, inositol 1,4,5-trisphosphate, and to calcium ions. *Proc. Natl. Acad. Sci. USA* **86,** 2708–2712
40. Wilkins, M., and Sneyd, J. (1998) Intercellular spiral waves of calcium. *J. Theor. Biol.* **191,** 299–308
41. Murray, J. (1989) *Mathematical Biology,* Springer, Berlin.
42. Motta, P. M. (1988) *Biopathology of The Liver. An Ultrastructural Approach.* (Motta, P. M. ed.) Kluwer Academic Publishers, Dordrecht
43. Jafri, M., and Keizer, J. (1994) Diffusion of inositol 1,4,5-trisphosphate, but not Ca^{2+}, is necessary for a class of inositol 1,4,5-trisphosphate-induced Ca^{2+} waves. *Proc. Natl. Acad. Sci. USA* **91,** 9485–9489
44. Keener, J., and Sneyd, J. (1999) *Mathematical Physiology.* Springer-Verlag, New York
45. Lindqvist, S. M., Sharp, P., Johnson, I. T., Satoh, Y., and Williams, M. R. (1998) Acetylcholine-induced calcium signaling along the rat colonic crypt axis. *Gastroenterology* **115,** 1131–1143

Received for publication March 22, 1999.
Revised for publication September 23, 1999.